51st IEEE Conference on Decision and Control
December 10-13, 2012. Maui, Hawaii, USA

A Fractional Order Maximum Power Point Tracker: Stability Analysis and Experiments

Hadi Malek, *Student Member, IEEE*, Sara Dadras, *Student Member, IEEE*, YangQuan Chen, *Senior Member, IEEE*

Abstract— **This paper presents a fractional order extremum seeking control scheme for maximum power point tracking tasks to better accommodate rapid varying solar irradiance for photovoltaic (PV) arrays. The stability analysis of the proposed control algorithm is presented first. Then the new algorithm is benchmarked against the integer order extremum seeking control. Our extensive simulation and experimental results show that, our proposed maximum power point tracker has faster convergence speed in comparison with integer order one.**

I. Introduction

Solar energy represents a key opportunity for increasing the role of renewable energy in the electric grid. Recently, Photo-Voltaic (PV) array system is likely recognized and widely utilized to the forefront in electric power applications. It can generate direct current electricity without environmental impact and contamination when is exposed to solar radiation.

Generally, PV sources exhibit nonlinear voltage-current and voltage-power characteristics as shown in Fig. 1 and their power output mainly depends on the nature of the connected load. Hence direct load connection to the PV system results in poor overall efficiency. However, maximum power extraction is achievable by substituting the direct load connection with an intermediate converter between load and PV panel. By using Maximum Power Point Tracking algorithms (MPPT), this converter can adaptively control the current (or voltage) and consequently power, based on their effective conditions such as load characteristics and environmental conditions.

Tracking the Maximum Power Point (MPP) of a photovoltaic array is usually an essential part of a PV system. Many MPP tracking methods have been developed and implemented which are different in some aspects like complexity, sensors required, convergence speed, cost and etc.

Hadi Malek, Researcher, Utah State Research Foundation (USURF), 1695 North Research Park Way, North Logan, USA (Phone: 801-688-6623; e-mail: hadi.malek@ieee.org).

Sara Dadras is with CSOIS, ECE Department, Utah State University, Logan, UT, USA, on leave from Tarbiat Modares University, Tehran, Iran (e-mail: s_dadras@ieee.org).

YangQuan Chen, Associate Professor, Dep. of Electrical and Computer Engineering Department, Director of CSOIS, Utah State University, 4120 Old Main Hill, Logan, UT 84322-4120, USA, (Phone: 435-797-0148; e-mail:yqchen@ieee.org, W:http://mechatronics.ece.usu.edu/yqchen/).

Among all the papers on this issue, much focus has been on perturb and observe (P&O) [1-3] method. Perturb and observe is a workhorse MPPT algorithm because of its trade off between performance and simplicity [4]. In its simplest form, the P&O scheme tracks the MPP by perturbing the input voltage (or current) in a given direction and observing if the output power increase or decrease. Reduction in output power leads to change (reverse) input direction but increase in power output results the same perturbation direction. It has been demonstrated that P&O tracks in the wrong direction given rapidly varying irradiance [5].

Recently, a promising new MPPT algorithm, called Extremum Seeking (ES) control, has been introduced to solve this problem. The ES method of Krstic [6] offers fast convergence and good steady-state performance with guaranteed stability for a range of parameters. This method not only improves the performance of MPPT but also is more robust against parameter variations [6]. In this method, the system is perturbed using an external excitation signal to compute the gradient. The framework of ES allows the use of unknown objective functions. This technique has been proven useful for PV application.

In this paper, fractional order operators have been combined by ES algorithm to improve the convergence speed of this algorithm. This combination transfers the benefits of robustness and stability of fractional order systems to the ES method.

The rest of the paper is organized as follows: Section II presents the integer order extremum seeking scheme. In Sections III, the proposed fractional order extremum seeking control is introduced together with its stability analysis. Simulation and experimental results is compared in section IV and V. Finally, some concluding remarks are drawn in Section VI.

II. Integer Order Extremum Seeking Control

To maximize the PV array power output, we employ a simple yet widely studied Integer Order Extremum Seeking (IOES) scheme [6,10] (Fig. 2) for static nonlinear maps, shown in Fig. 1, The control scheme applies a periodic perturbation $a_0 \sin(\omega t)$ to the duty ratio signal $\hat{d}$, which is the current estimate of the optimum duty ratio d^*. Assuming the boost DC/DC converter dynamics can be approximated as instantaneous [11], the sinusoidal varying duty ratio imposes a sinusoidal varying input voltage. This voltage passes through the static nonlinearity $f(\hat{d} + a_0 \sin(\omega t))$,

representing the PV array's *P-V* characteristic curve, to produce a periodic power output *p*.

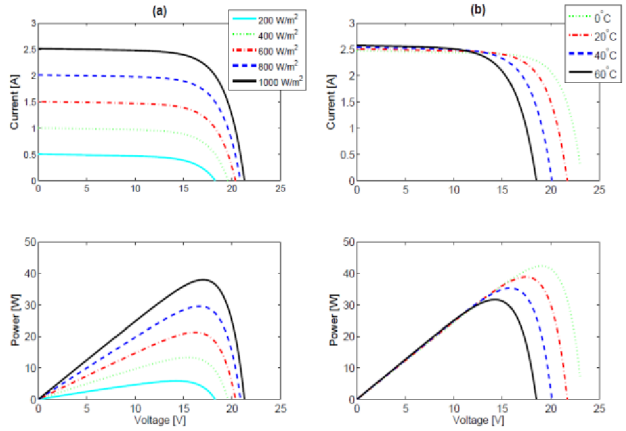

Figure 1: Characteristic I-V and P-V curves for (a) varying irradiation levels and T = 25°C, (b) varying temperature levels and S = 1000W/m^2.

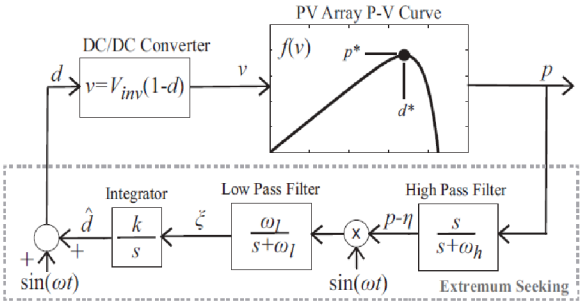

Figure 2: Block diagram of proposed integer order extremum seeking control system [12].

The high-pass filter $s/(s+\omega_h)$ then eliminates the DC component of *p*, and will be in phase or out of phase with the perturbation signal $a_0\sin(\omega t)$ if $\hat{d}$ is less than or greater than d^*, respectively. This property is important, because when the signal η is multiplied by the perturbation signal $\sin(\omega t)$, the resulting signal has a DC component that is greater than or less than zero if $\hat{d}$ is less than or greater than d^*, respectively. This DC component is then extracted by the low-pass filter $\omega_l/(s+\omega_l)$. Therefore, the signal ξ can be thought of as the sensitivity $(a_0^2/2)\frac{\partial f}{\partial d}(\hat{d})$ and we may use the gradient update $\dot{\hat{d}} = k(a_0^2/2)\frac{\partial f}{\partial d}(\hat{d})$ to force $\hat{d}$ to converge to d^* and control goal is achieved.

III. Fractional Order Extremum Seeking Control

In this part, first the Fractional Order Extremum Seeking Control (FOESC) scheme is presented and then the stability of this method is investigated.

A. Fractional Order Extremum Seeking Control Scheme

A fractional order extremum seeking approach, shown in Fig. 3, is presented. In this approach the integer order integrator of IOESC is replaced by a fractional order integrator. As we will show later, this replacement can improve the convergence speed of ESC algorithm.

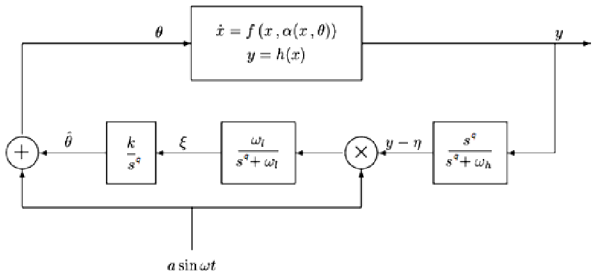

Figure 3: An FOESC scheme

Consider a general SISO nonlinear model

$$\begin{aligned} \dot{x} &= f(x,u) \\ y &= h(x) \\ u &= \alpha(x,\theta) \end{aligned} \tag{9}$$

Assumption 1: There exists a smooth function $l: R \to R^n$ such that

$$\begin{aligned} &f(x,\alpha(x,\theta)) = 0 \\ &\qquad if\ and\ only\ if\ x = l(\theta) \end{aligned} \tag{10}$$

Assumption 2: For each $\theta \in R$, the equilibrium $x = l(\theta)$ of the system $\dot{x} = f(x,\alpha(x,\theta))$ is locally exponentially stable with decay and overshoot constants uniform in θ.

Assumption 3: There exists $\theta^* \in R$ such that

$$\begin{aligned} &(h\circ l)'(\theta^*) = 0 \\ &(h\circ l)''(\theta^*) < 0 \end{aligned} \tag{11}$$

Where (.)' and (.)" are the first and second derivative operators.

Based on Figure 5 and without loss of generality we assume that the cut of frequency of fractional order filters are the same as integer order filers, we have

$$\begin{aligned} &\dot{x} = f(x, \alpha(x, \hat{\theta} + a\sin(\omega t))), \\ &D^q\hat{\theta} = k\,\xi, \\ &D^q\xi = -\omega_l\xi + \omega_l(y-\eta)a\sin(\omega t), \\ &D^q\eta = -\omega_h\eta + \omega_h y. \end{aligned} \tag{12}$$

where D^q is the fractional order Reimann-Liouville integrator [13].

B. Stability of Fractional Order Extremum Seeking Control

Let us introduce new coordinates

$$\begin{aligned}\tilde{\theta} &= \hat{\theta} - \theta^* \\ \tilde{\eta} &= \eta - h \circ l(\theta^*)\end{aligned} \tag{13}$$

Then, in the time scale $\tau = \omega t$, the aforementioned system is rewritten as

$$\begin{aligned}\omega \frac{dx}{d\tau} &= f\,(x, \alpha(x, \theta^* + \tilde{\theta} + a\sin(\tau))) \\ \frac{d^q}{d\tau^q}\begin{bmatrix}\tilde{\theta}\\ \xi\\ \tilde{\eta}\end{bmatrix} &= \delta\begin{bmatrix} k\,\xi \\ -\omega_L'\xi + \omega_L'(h(x) - h\circ l(\theta^*) - \tilde{\eta})a\sin(\tau) \\ -\omega_H'\tilde{\eta} + \omega_H'(h(x) - h\circ l(\theta^*))\end{bmatrix}\end{aligned} \tag{14}$$

Where $D^q = \dfrac{d^q}{dt^q}$.

For the stability analysis, we need to freeze "x" in its equilibrium value

$$x = l(\theta^* + \tilde{\theta} + a\sin(\tau)) \tag{16}$$

Then, we have

$$\frac{d^q}{d\tau^q}\begin{bmatrix}\tilde{\theta}_r\\ \xi_r\\ \tilde{\eta}_r\end{bmatrix} = \delta\begin{bmatrix} k\,\xi_r \\ -\omega_L'\xi_r + \omega_L'(v(\tilde{\theta}_r + a\sin(\tau)) - \tilde{\eta}_r)a\sin(\tau) \\ -\omega_H'\tilde{\eta}_r + \omega_H' v(\tilde{\theta}_r + a\sin(\tau))\end{bmatrix} \tag{17}$$

where $(.)_r$ means reduced system and,

$$\begin{aligned}v(\tilde{\theta}_r + a\sin(\tau)) &= h\circ l(\theta^* + \tilde{\theta}_r + a\sin(\tau)) \\ &\quad - h\circ l(\theta^*)\end{aligned} \tag{18}$$

Using assumption 3, one can easily conclude

$$\begin{aligned}&v(0) = 0, \\ &v'(0) = (h\circ l)'(\theta^*) = 0, \\ &v''(0) = (h\circ l)''(\theta^*) < 0.\end{aligned} \tag{19}$$

Now, using the averaging method [14], we have

$$\begin{aligned}\frac{d^q}{d\tau^q}\begin{bmatrix}\tilde{\theta}_r^a\\ \xi_r^a\\ \tilde{\eta}_r^a\end{bmatrix} &= \\ \delta\begin{bmatrix} k\,\xi_r^a \\ -\omega_L'\xi_r^a + \dfrac{\omega_L'}{2\pi}a\displaystyle\int_0^{2\pi} v(\tilde{\theta}_r^a + a\sin(\sigma))\sin(\sigma)d\sigma \\ -\omega_H'\tilde{\eta}_r^a + \dfrac{\omega_H'}{2\pi}\displaystyle\int_0^{2\pi} v(\tilde{\theta}_r^a + a\sin(\sigma))d\sigma\end{bmatrix}\end{aligned} \tag{20}$$

First, we need to determine the average equilibrium $(\tilde{\theta}_r^{a,e}, \xi_r^{a,e}, \tilde{\eta}_r^{a,e})$ which satisfies

$$\begin{aligned}\xi_r^{a,e} &= cte, \\ \xi_r^{a,e} &= \frac{1}{2\pi}\int_0^{2\pi} v(\tilde{\theta}_r^{a,e} + a\sin\sigma)\sin\sigma\, d\sigma \\ \tilde{\eta}_r^{a,e} &= \frac{1}{2\pi}\int_0^{2\pi} v(\tilde{\theta}_r^{a,e} + a\sin\sigma)d\sigma\end{aligned} \tag{21}$$

Then

$$\begin{aligned}\xi_r^{a,e} &= cte, \\ \xi_r^{a,e} &= \frac{1}{2\pi}\int_0^{2\pi} v(\tilde{\theta}_r^{a,e} + a\sin\sigma)\sin\sigma\, d\sigma \\ \tilde{\eta}_r^{a,e} &= \frac{1}{2\pi}\int_0^{2\pi} v(\tilde{\theta}_r^{a,e} + a\sin\sigma)d\sigma\end{aligned} \tag{22}$$

By postulating $\tilde{\theta}_r^{a,e}$ in the form

$$\tilde{\theta}_r^{a,e} = b_1 a + b_2 a^2 + O(a^3), \tag{23}$$

we get

$$\begin{aligned}&v''(0)b_1 = 0, \\ &v''(0)b_2 + \frac{1}{8}v'''(0) = 0\end{aligned} \tag{24}$$

which implies

$$\tilde{\theta}_r^{a,e} = -\frac{v'''(0)}{8v''(0)}a^2 + O(a^3). \tag{25}$$

This results in

$$\tilde{\eta}_r^{a,e} = \frac{v''(0)}{4}a^2 + O(a^3). \tag{26}$$

Thus, the equilibrium of the average model is

$$\begin{bmatrix}\tilde{\theta}_r^{a,e}\\ \xi_r^{a,e}\\ \tilde{\eta}_r^{a,e}\end{bmatrix} = \delta\begin{bmatrix} -\dfrac{v'''(0)}{8v''(0)}a^2 + O(a^3) \\ 0 \\ \dfrac{v''(0)}{4}a^2 + O(a^3)\end{bmatrix}. \tag{27}$$

The Jacobian matrix at $(\tilde{\theta}, \xi, \tilde{\eta})_r^{a,e}$ for the above system is

$$J_r^a = \delta.\begin{bmatrix} 0 & k & 0 \\ \dfrac{\omega_L'}{2\pi}a\displaystyle\int_0^{2\pi} v'(\tilde{\theta}_r^{a,e} + a\sin(\sigma))\sin(\sigma)d\sigma & -\omega_L' & 0 \\ \dfrac{\omega_H'}{2\pi}\displaystyle\int_0^{2\pi} v'(\tilde{\theta}_r^{a,e} + a\sin(\sigma))d\sigma & 0 & -\omega_H'\end{bmatrix} \tag{28}$$

Since J_r^a is block-lower-triangular, it can be concluded that it will be Hurwitz if and only if

$$\int_0^{2\pi} v'(\tilde{\theta}_r^{a,e} + a\sin(\sigma))\sin(\sigma)d\sigma < 0 \tag{29}$$

So, from the previous parts, one can easily conclude

$$\int_0^{2\pi} v'\left(\tilde{\theta}_r^{a,e} + a\sin(\sigma)\right)\sin(\sigma)d\sigma = \pi v''(0)a + O(a^2) \tag{30}$$

Then, we get

$$\det(\lambda I - J_r^a) = \left(\lambda^2 + \delta\omega_L'\lambda - \frac{\delta^2\omega_L' K'}{2}v''(0)a^2 + O(\delta^2 a^3)\right) \times \left(\lambda + \delta\omega_H'\right) \tag{31}$$

which proves that J_r^a is Hurwitz for sufficiently small a. This, in turn, implies the equilibrium of the average system is exponentially stable for a sufficiently small a.

IV. Simulation Results

A. Simulation Results

In this section the IOESC and FOESC are applied to the PV model and boost DC-DC converter using Simulink/Matlab. The output of ESC block is used as the input for the converter to tune its duty cycle (Fig. 4).

Numerical simulations have been done in two cases: without and with environmental noise. The results are illustrated in Figs. 5 and 6. The simulations have been done under these conditions: T=25°C and G=1000 W/m^2 and the extremum seeking control gain equals to k=250. The applied noise to the model is a uniform noise ~U(-0.1,0.1).

Simulation results show that in both case, FOESC converges to the extremum point faster than the IOESC. Applied extremum seeking scheme performance is satisfactory regardless of whichever admissible noise affects the system.

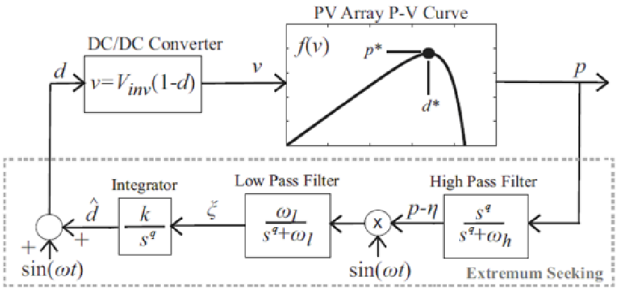

Figure 4: Block diagram of proposed fractional order extremum seeking control system.

To do more investigation regarding the role of the fractional integration order, more simulations have been done for a constant arbitrary k=150, while q (order of the fractional integrator) is changing in the range of 0.88 to 0.97. The results are presented in Fig. 7. According to these results, by reducing q, speed of convergence is increased.

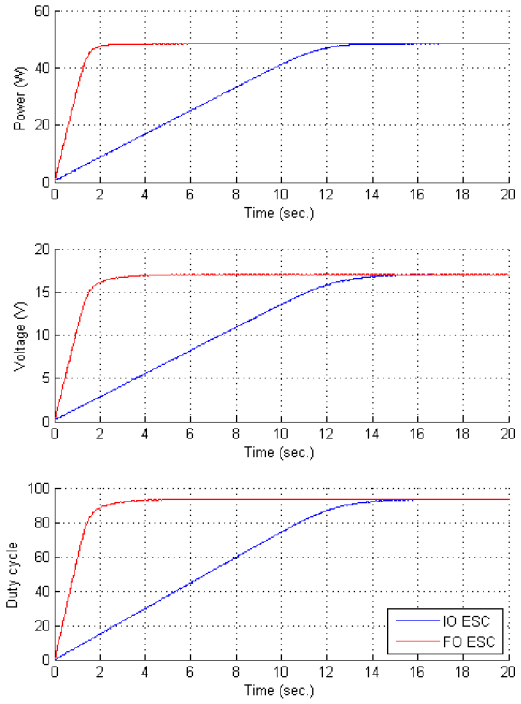

Figure 5: Time response of the PV Module without noise when fractional order ESC is applied (q=0.95).

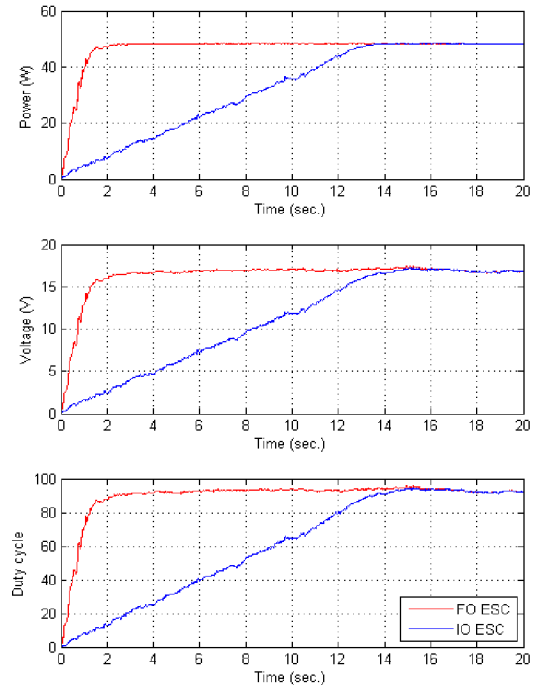

Figure 6: Time response of the PV Module in presence of noise when fractional order ESC is applied (q=0.95).

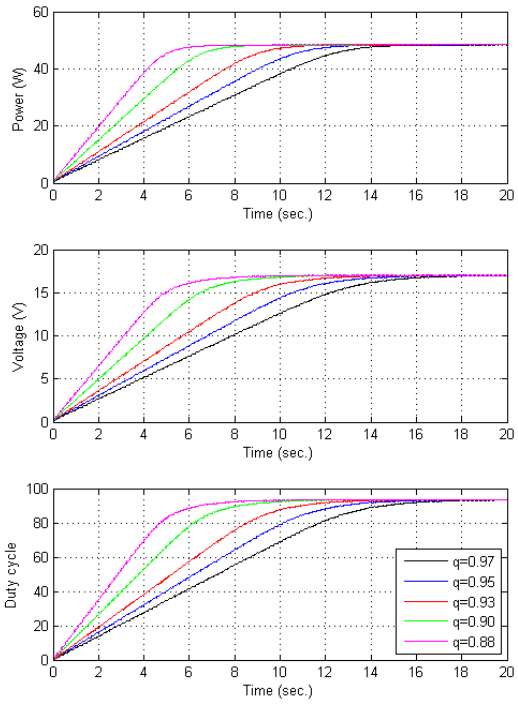

Figure 7: Time responses of the PV module for different integration orders in fractional order ESC.

V. Experimental Results

A. *Fractional Horsepower Dynamometer*

A fractional horsepower dynamometer is used to model the PV panel. The dynamometer includes a dc motor and hysteresis brake. Generally, brake is used for modeling any nonlinear plant (in this case PV panel behavior).

Without loss of generality, DC motor of dynamometer can be approximated by the following transfer function

$$G_m(s) = \frac{1.52}{1.01s + 1}. \tag{32}$$

Since the brake has a nonlinear behavior, we can adapt the PV panel behavior as a model for the hysteresis brake. In other words, the hysteresis brake acts as a PV. The proposed scheme can be seen in Fig. 8.

For this purpose, a fractional order horsepower dynamometer showed in Fig. 9 has been used. The Magtrol Hysteresis Brake used in the dynamometer produces torque strictly through an air gap, without the use of magnetic particles or friction components. This method of breaking provides far superior characteristics (smoother torque, longer life, superior repeatability, higher degree of controllability, and less maintenance and down time). Brake and motor are each driven by an advanced motion controls brush type PWM servo amplifier Model 50A8. These controllers receive analog signals from data acquisition hardware. The PWM controllers use these signals to set the voltage output to the motor or brake. The controller then supplies all the current needed to maintain the set voltage level [15].

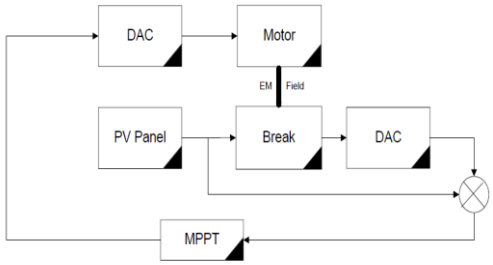

Figure 8: Modeling the PV panel using fractional horsepower dynamometer.

As mentioned in the pervious section, using fractional horsepower dynamometer, some experiments have been done to support the numerical simulation results. The results are consistent with the numerical results that have been achieved in the previous part. In other words, the PV can reach its maximum power point.

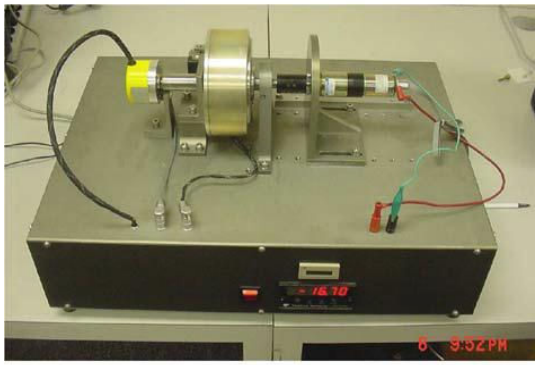

Figure 9: The fractional horse power dynamometer developed at CSOIS [15].

Extremum seeking control scheme is tested using the Matlab/Simulink environment, which uses the WinCon application, from Quanser, to communicate with the Quanser MultiQ3 data acquisition card. Simulink model used for the experiments is shown in Fig. 10.

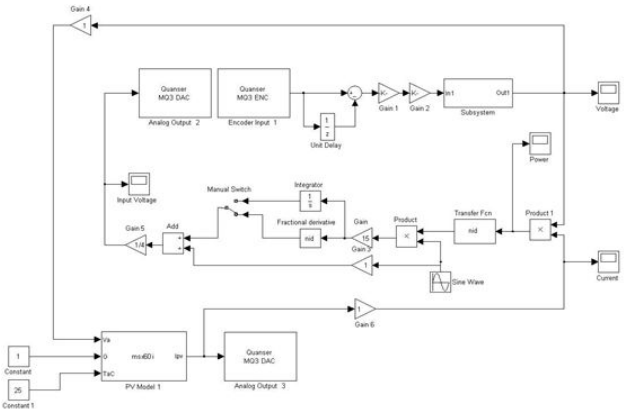

Figure 10: Simulink model used in the fractional order ESC real time experiments using RTW Windows Target.

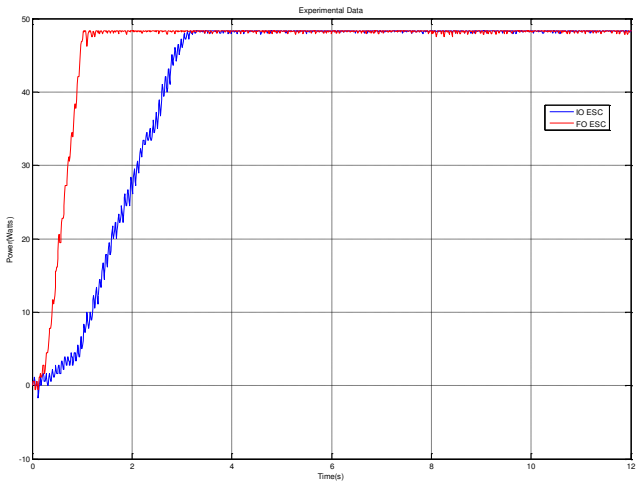

Figure 11: Convergence of PV power to extremum point applying IOESC and FOESC (q=0.95).

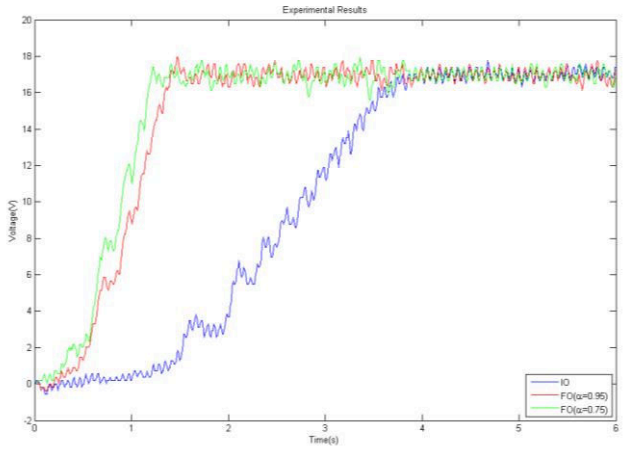

Figure 12: Convergence of PV voltage to extremum point applying different integration orders in IOESC and FOESC.

By using this architecture, proposed FOESC scheme can be easily applied to the fractional horsepower dynamometer as a PV model and the results are satisfactory.

Fig. 11 represents the convergence speed of FOESC and also IOESC which admits the results achieved from numerical simulation results in previous part.

Figure 12 illustrates order reduction effect of fractional order extremum seeking method which can improve the convergence speed of FOESC.

VI. Conclusion

One of the most important parameters in all MPPT architectures is convergence speed. Brunton has pointed out in his paper, "As irradiance decreases rapidly, the I–V curve shrinks and the MPV and MPI decrease. If the MPPT algorithm does not track fast enough, the control current or voltage will fall off the I–V curve." [4]. Therefore any improvement in the rise time of MPPT is mostly desirable and will improve the reliability of MPPT device.

In this paper, a PV model, IO and FO ESC schemes is briefly introduced. Using Simulink/Matlab, the proposed extremum seeking control method with both integer order and fractional order operators are applied to a PV model in two cases: in presence of environmental noise and without noise. Then using fractional horsepower dynamometer, as a benchmark, to model nonlinear behavior of PV panel, some experiments have been done to test the introduced fractional order extremum seeking algorithm.

From the experimental results, it can also be declared that the fractional order ESC has a better performance in comparison with integer order ESC with regard to convergence speed.

Also stability of this algorithm has been investigated to show the effectiveness of this algorithm and to assure it can work properly without making the whole system unstable.

References

[1] O. Wasynczuk, "Dynamic behavior of a class of photovoltaic power systems," IEEE Trans. Power App. Syst., vol. 102, pp. 3031-3037, Sept. 1983.

[2] C. Hua and J. R. Lin, "DSP-based controller application in battery storage of photovoltaic system," in Proc. 1996 IEEE IECON 22nd International Conf. on Ind. Electron., Contr., and Instrum., 1996, pp. 1705-1710.

[3] N. Kasa, T. Iida, and L. Chen, "Flyback Inverter Controlled by Sensorless Current MPPT for Photovoltaic Power System," IEEE Trans. Ind. Electron., vol. 52, pp. 1145-1152, Aug. 2005.

[4] S.L. Brunton, C.W. Rowley, S. R. Kulkarni, C. Clarkson, " Maximum power point tracking for photovoltaic optimization using Ripple-Based extremum seeking," IEEE Transactions On Power Electronics, Vol. 25, pp. 2531-2540, 2010.

[5] T. Esram and P. L. Chapman, "Comparison of photovoltaic array maximum power point tracking techniques," IEEE Transactions On Energy Conversion, vol. 22, pp. 439–449, 2007.

[6] K. Ariyur and M. Krstic, *Real Time Optimization by Extremum Seeking Control,* Wiley, 2003.

[7] CIGRE TF38.01.10 "Modeling New Forms of Generation and Storage", November 2000.

[8] F.M. González-Longatt, "Model of Photovoltaic Module in Matlab™," 2do Congreso Iberoamericano de Estudiantes de Ingenieria electrica, Electronica y Computacion, CIBELEC, 2005.

[9] J. A. Gow, C. D. Manning "Development of a photovoltaic array model for use in power electronics simulation studies," IEEE Proceedings on Electric Power Applications, vol. 146, no. 2, pp. 193-200, March 1999.

[10] M. Krstic and H.H. Wang, "Stability of extremum seeking feedback for general nonlinear dynamic systems," Automatica, vol. 36, no. 4, pp. 595-601, 2000.

[11] B. Johansson, "Improved Models for DC-DC Converters," Department of Industrial Electrical Engineering and Automation, Lund University, 2003.

[12] S. .Moura, "A switched extremum seeking approach to maximum power point tracking in photovoltaic systems," EECS 498-003 Project, April 2009.

[13] I. Polubny, *Fractional differential equations*. New York: Academic Press, 1999.

[14] H. K. Khalil, Nonlinear systems. Prentice Hall Upper Saddle River, NJ, 2002.

[15] Y. Tarte, Y.Q. Chen, W. Ren, and K. Moore, "Fractional horsepower dynamometer-A general purpose hardware-in-the-loop real-time simulation platform for nonlinear control research and education", Proc. 45th IEEE Conference on Decision and Control, San Diego, 2006, pp. 3912-3917.